Bose–Einstein Condensation in Atomic Gases

J. Zachorowski and W. Gawlik

M. Smoluchowski Institute of Physics, Jagellonian University
Reymonta 4, 30-059 Kraków, Poland

This paper presents fundamental principles, characteristics, and limitations of various experimental methods of cooling and trapping of neutral atoms by laser light and magnetic fields. In addition to surveying the experimental techniques, basic properties of quantum degenerate gases are discussed with particular emphasis on the Bose–Einstein condensate. We also present main parameters and expected characteristics of the first Polish Bose–Einstein condensate apparatus built in the National Laboratory of Atomic, Molecular, and Optical Physics in Toruń, Poland.

PACS numbers: 03.75.Fi, 32.80.Pj, 39.25.+k

1. Introduction

Bose–Einstein condensation is a peculiar phenomenon of quantum degeneracy characteristic of non-interacting Bose particles at sufficiently low temperature and high density.

The achieving of the Bose–Einstein condensation in atomic gases has been awarded with Nobel Prize for E. Cornell, W. Ketterle, and C. Wieman in 2001 but its roots are more than 75 years older. In 1924, Satyendranath Bose [1] derived Planck's law from the principles of statistical physics and in 1925 Albert Einstein [2] generalized that work to mass-particles and discovered the existence of the phase transition at low temperatures which is now known as the Bose–Einstein condensation. The idea remained abstract for a long time even for the authors; Einstein himself wrote: *The theory is pretty but is there also some truth to it?*

(577)

2. Basic principles

Bose–Einstein condensation (BEC) can be analyzed from two different perspectives: (a) statistical physics and (b) matter waves of quantum degenerate particles.

2.1. Statistical picture

Starting from the partition function for bosons in temperature T

$$f(\epsilon) = \frac{1}{\exp \beta(\epsilon - \mu) - 1},$$ (1)

where ϵ stands for the particle energy, μ is the chemical potential, and $\beta = 1/k_{\rm B}T$ ($k_{\rm B}$ being the Boltzmann constant), and using the normalization condition $N = \sum_\epsilon f(\epsilon)$, one can express the total number of particles as

$$N = N_0 + \int_0^\infty f(\epsilon)\rho(\epsilon)\mathrm{d}\epsilon.$$ (2)

N_0 denotes here the number of particles in the ground state, and $\rho(\epsilon)$ represents density of energy states. Below a certain critical temperature, the integral in Eq. (2) becomes much smaller than N, i.e., most of particles are in the ground state. This populating of the ground state occurs as a phase transition at a critical temperature, as visualized in Fig. 1.
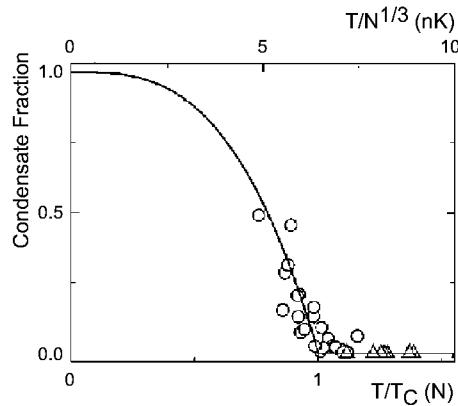

Fig. 1.   Solid line shows population of atomic ground state versus temperature in units of critical temperature $T_{\rm c}$ ($T_{\rm c}$ depends on atomic density N). Circles are experimental results from [3] (reproduced with kind permission of the authors).

2.2. Matter wave picture

The de Broglie wavelength of the particles depends on their momentum, and therefore, on temperature. It is given by $\lambda_{\rm dB} = (2\pi\hbar^2/mk_{\rm B}T)^{1/2}$. In a medium of

particle density n and mean distance between particles $n^{-1/3}$, the indistinguisha-bility of quantum objects becomes important when the de Broglie wavelength becomes comparable to the inter-particle distance, $n^{-1/3} \approx \lambda_{dB}$. One speaks then about quantum degeneracy, i.e., about B–E condensation for bosonic particles. In principle, this condition can be achieved either by increasing the de Broglie wavelength (decrease in temperature) or by decreasing the distance between par-ticles (increase in density). The two solutions are not equivalent as the latter enhances the inter-particle interactions and one cannot speak any more of free particles. It is instructive to compare orders of magnitude typical of the thermal and condensed gas samples. For atom gas at a temperature of 900 K with a density $n \approx 10^{16}$ cm^{-3} and mean distance $n^{-1/3} \approx 10^{-7}$ m, $\lambda_{dB} \approx 10^{-12}$ m. One has in this case $\lambda_{dB} \ll n^{-1/3}$. On the other hand, with about $N = 10^4$ cold atoms in a trap at a temperature $T \approx 100$ nK, $\lambda_{dB} \approx n^{-1/3}$, i.e., quantum degeneracy occurs.

Note that for treating an atom as a boson or fermion, the statistical proper-ties of an atom as a whole need to be taken into account. An atom can be a boson or fermion depending on the total number of its fermionic constituents: electrons and nucleons, therefore, different isotopes of the same element may have different statistical properties, as discussed in Sec. 9 for lithium. Additionally, for trapped atoms the energy levels are quantized with a level distance given by the trap fre-quency ω. The condensation occurs at temperature much higher than the level spacing, $k_B T \gg \hbar\omega$, and in this context Bose–Einstein condensation is a "high temperature effect".

3. History

The history of the quest for the Bose–Einstein condensation has three main streams connected with studies of superfluidity, advances in cooling, and trapping of neutral atoms, and efforts to achieve BEC in atomic hydrogen. Let us briefly recall the milestones of each.

3.1. "Cryogenic route"

- Discovery of superfluidity in ^{4}He at 2.17 K by H. Kammerlingh Onnes awarded with Nobel Prize in 1913.

- Suggestion by F. London that superfluidity is a manifestation of BEC (1938).

- L.D. Landau theory of superfluidity (1941), Nobel 1962.

- Theory of O. Penrose and L. Onsager (1950s) describing a long-range order in the highly correlated bosonic system. Calculation of the condensate fraction in superfluid ^{4}He — only 8% of atoms,

- N.N. Bogoliubov's calculation of a low-energy phonon spectrum (1947).

- Phase transition in ^{3}He at 3 mK discovered by D.M. Lee, D.D. Osheroff, and R. Richardson in 1972, Nobel 1996.

It should be pointed out that He is not an ideal gas when it shows superfluidity, the strong interaction between atoms is the reason for only 8% condensate fraction.

3.2. Cooling and trapping of neutral atoms

- 1968–70 V.S. Letokhov and A. Ashkin presented the first ideas of trapping atoms in light fields,

- 1975 T.W. Hänsch and A.L. Schawlow proposed the method of cooling of atoms by light,

- around 1980 V.L. Balykin, V.S. Letokhov, and W.D. Phillips performed first experiments,

- S. Chu and W.D. Phillips demonstrated the first optical and magnetic traps,

- 1986 J. Dalibard, D.E. Pritchard, and S. Chu developed the magneto-optical trap,

- 1997 W.D. Phillips, S. Chu, and C. Cohen-Tannoudji awarded with Nobel Prize for development of cooling methods.

3.3. Quest for BEC in atomic hydrogen

The search for BEC in hydrogen was dictated by the desire to study a medium that remains in a gas phase even at the lowest temperatures.

- 1976 L.H. Nosanov and W.C. Stwalley discovered that polarized hydrogen did not solidify (ground state of H_2, $S = 0$, is not accessible by spin-polarized H atoms),

- 1976 experiments performed by D. Kleppner and T.J. Greytak (MIT) and by I.F. Silvera and J. Walraven (Amsterdam),

- 1986 H.F. Hess developed evaporation cooling technique.

4. How to cool atoms?

4.1. Cooling of atomic beam

Let us start by showing the possibility of stopping the atomic beam. Consider a beam of atoms and a counter-propagating laser beam at a frequency of the atomic resonance (Fig. 2). Absorption of a photon by an atom leads to an atomic transition to a higher energetic state, but also changes the atomic momentum by the photon momentum $\hbar k_L$, k_L being the wave vector. The subsequent relaxation to the ground energetic state by spontaneous emission also changes the atomic momentum. There is asymmetry between these two processes due to the fact that
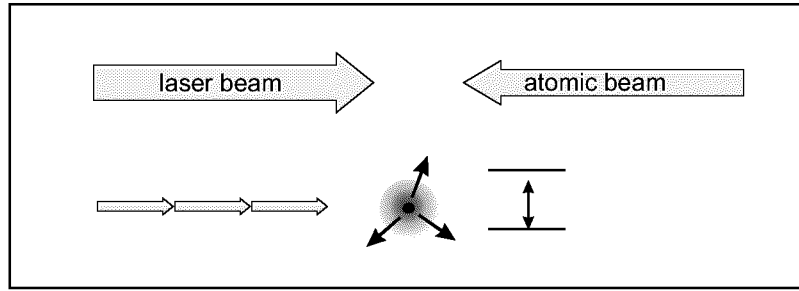
Fig. 2. Principle of laser deceleration of collimated atomic beams. Laser photons arrive from a well-defined direction, whereas spontaneously emitted photons are essentially isotropic. The momenta of absorbed laser photons are therefore accumulating to a nonzero value, while the net momentum change in spontaneous emission is zero. This gives rise to a light-pressure force in a direction of a laser beam.

all absorbed photons have equal wave vectors, whereas the spontaneously emitted photons have an arbitrary direction. Therefore a total momentum transfer after N absorption–emission cycles is

$$\Delta p = \sum \hbar k_{\mathrm{abs}} - \sum \hbar k_{\mathrm{em}} = N \hbar k_L - 0. \tag{3}$$

As an example let us take sodium atoms with the mass number $M = 23$ and mean velocity at 400 K $v = 600$ m/s, illuminated with laser of $\lambda = 590$ nm. Each photon causes only a minimal change of atomic velocity so that one needs some 20 000 photon absorptions to stop an atom. At a quite modest laser beam intensity of $I = 6$ mW/cm^2 it can be done very fast. An atom can be stopped in 1 ms, on a distance of 0.5 m with a deceleration achieving 10^6 m/s^2.

4.2. Cooling of atomic gas

For the case of gas contained in a cell, one has atoms moving in arbitrary directions and thus to cool them along e.g. x axis, one has to use two
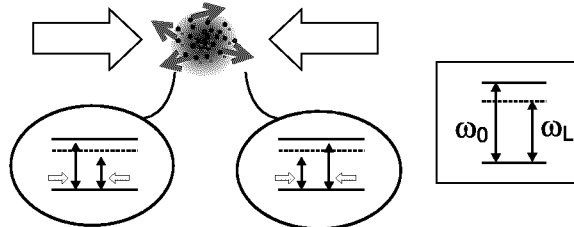

Fig. 3. Principle of 1D laser cooling of atomic gas. The two counter-propagating laser beams of equal intensities have their frequencies ω_L below the atomic resonance frequency ω_0. Due to Doppler effect, a moving atom experiences a nonzero force that slows its movement no matter in which direction.

counter-propagating beams propagating along the OX direction, of the same frequency ω_L tuned below the frequency of the atomic transition, $\omega_L < \omega_0$ (Fig. 3). For such laser frequency, Doppler effect tunes atoms to resonance with beams propagating in the direction opposite to the atom velocity. Therefore, the force exerted by this beam (stopping force) will be bigger than the force from the counter-propagating beam (accelerating force) and the net effect would be slowing down of all atoms, i.e., cooling them.
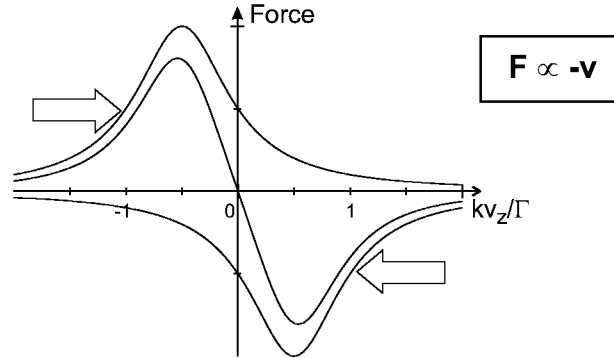

Fig. 4. The light pressure forces versus atomic velocity in k/Γ units (Γ is the spontaneous emission rate) for the case of $\omega_L - \omega_0 = \Gamma/2$. The forces associated with the two beams of Fig. 3 cancel for atoms with the zero velocity component. Around $v_z = 0$, the force has the velocity dependence typical of motion in viscous media.

The same process can be analyzed from the energetic point of view where one notes that less energy is absorbed than reemitted, which leads to cooling of atoms. Figure 4 shows the forces acting on atom produced by two counter-propagating laser beams and their sum versus atomic velocity. For a range of velocities close to zero, the effective force is proportional to velocity with a negative coefficient. It has thus a character of a viscous force. Such a configuration has thus been termed *optical molasses*.

The described one-dimensional cooling can be easily generalized for a three--dimensional case by adding another two pairs of counter-propagating laser beams. The atoms in the crossing point of all the beams are decelerated (cooled), yet they are not held by any force and can slowly diffuse from the light beams.

5. How to trap cold atoms?

To hold atoms in a prescribed spatial position (to trap them) one needs a position-dependent force. The most popular solution is the magneto-optical atomic trap (MOT), which combines the three-dimensional optical molasses configuration

of three pairs of anti-parallel laser beams tuned below the atomic resonance frequency with an inhomogeneous magnetic field of quadrupole configuration and proper circular polarization of the light beams. This produces a light force, which, apart from the velocity characteristics $F(v) \propto -v$ leading to atom cooling, has the desired spatial characteristics, $F(x) \propto -x$.
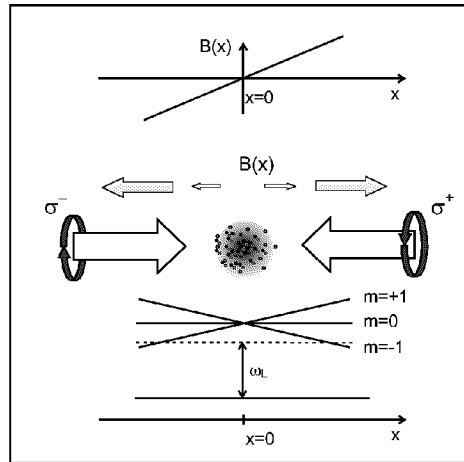

Fig. 5. Principle of a 1D magneto-optical trap. Atoms with $J_g = 0$ and $J_e = 0$ are placed in a magnetic field that depends linearly on position (top of the figure). Two counter-propagating beams, detuned below ω_0, are circularly polarized in opposite senses and induce transitions between different magnetic sublevels. Inhomogeneous magnetic field causes position dependent Zeeman shifts of the sublevels (lower part of the figure) such that an atom experiences position dependent light pressure. An atom displaced out of the zero-field position experiences a force which pushes it back to $x = 0$. Around the center, the net force is the same as in a harmonic trapping potential, $F(x) \propto -x$.
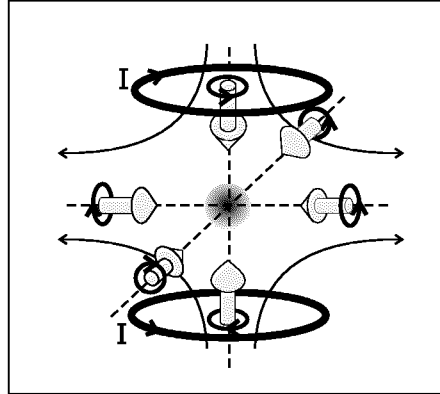

Fig. 6. A 3D realization of the magneto-optical trap. The quadrupole, inhomogeneous magnetic field is created by two anti-Helmholtz coils where current I flows in opposite directions.

It should be noted that the trapping forces are of optical, not magnetic, origin; the role of magnetic field is merely to control the intensity of optical forces in dependence on the spatial position. This is done by tuning atomic levels into, or out of, resonance with laser beams by the Zeeman shift of atomic levels, as shown in Fig. 5 for the one-dimensional case. The three-dimensional configuration of a MOT is presented in Fig. 6. It shows two anti-Helmholtz coils with opposite currents producing the quadrupole field and six laser beams with appropriate polarizations.

Atoms with nonzero angular momenta can be localized also in purely magnetic traps (MT), but such traps provide much weaker confinement and are thus suited only for much colder atoms (unless very high field gradients are used).

6. Temperature limits

Cooling of atoms by interaction with light beams has natural constraints that dictate the final achievable temperature. The cooling process is based on a momentum transfer process and dissipation of energy in cyclic processes of absorption and spontaneous emission. This leads to the decrease in average atomic velocity, which tends to zero. At the same time, however, the velocity dispersion is not zero and even increases. This increase in velocity dispersion (equivalent to heating) is caused by the momentum diffusion during consecutive absorption and emission acts. The final temperature is achieved when cooling and heating processes equalize. For a two-level atom, the limit temperature, T_D, depends only on the rate of atomic spontaneous emission rate, Γ and not on the single photon momentum $k_B T_D = \hbar \Gamma / 2$. T_D is the so-called "Doppler limit" temperature and equals 240 μK for Na atoms and 140 μK for Rb. When multi-level atomic structure is taken into account, additional cooling mechanisms become important (Sisyphus cooling), which lower the limit temperature to the sub-Doppler temperatures of $10-100$ μK.

On the other hand, the radiation imprisonment, i.e., reabsorption of spontaneously emitted photons in the dense atomic cloud leads to the density limit, $n_{max} = 10^{11}-10^{12}$ at/cm^3.

To reach yet lower temperatures of the order of 100 nK, needed for the BEC, it is necessary to switch all the light beams off and hold atoms in darkness in purely magnetic traps. As the magnetic forces are conservative, another cooling mechanism must be invoked. The required cooling is done by a forced evaporation of most energetic atoms. They are subjected to radio-frequency field, transferring atoms to another magnetic state, which is not trapped by the magnetic field configuration (Fig. 7). The remaining atoms should thermalize to lower temperature. This happens indeed, if the rate of collisions between atoms leading to thermalization is high enough, while the rate of other collisions, which could expel cold atoms from the trap, is so low as to provide enough time for the thermalization
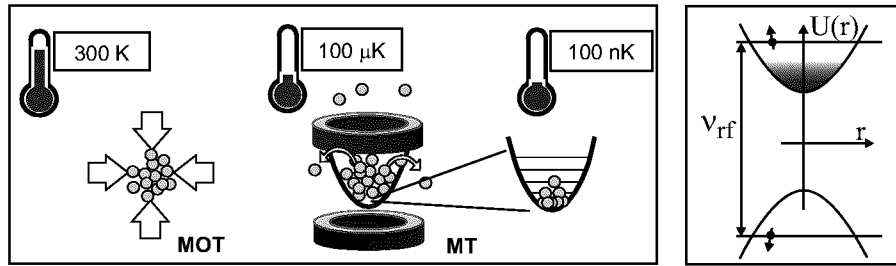
Fig. 7. Cooling atoms to the lowest temperatures. In the first stage MOT is used to bring atom gas from a room temperature to about 100 mK. Next, a magnetic trap is used and atoms are cooled further by a forced evaporation below 100 nK. In the right figure, the mechanism of evaporation is depicted: radio-frequency field is resonant with a transition between given levels within the trapping and anti-trapping potential surfaces of the magnetic trap and can drive atoms of a given energy out of the trap. By lowering the transition frequency, less energetic atoms in a trap are addressed. After each evaporation step, the remaining atoms are allowed to thermalize so that they can reach equilibrium distribution with appropriately lower temperature.

process. The evaporative cooling technique invented for the case of hydrogen has been fruitfully applied to other elements as well.

7. Achieving Bose–Einstein condensation

The standard way to achieve Bose–Einstein condensation of atomic gases consists of three steps:
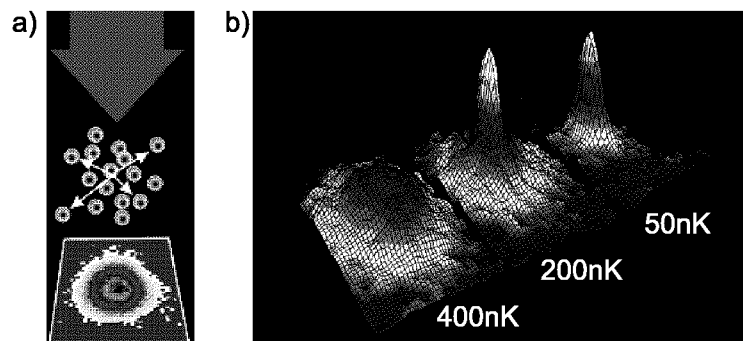

Fig. 8. (a) Idea of imaging of trapped atoms by recording their shadow caused by a resonant light absorption. (b) First observation of the BEC with ultra-cold ^{87}Rb atoms in a magnetic trap [4] (courtesy of the JILA BEC group). Three distributions correspond to different temperatures reached by the evaporation method.

1. collection of atoms in a magneto-optical trap and cooling by laser interaction to sub-Doppler temperatures,

2. transfer of pre-cooled to the magnetic trap,

3. evaporative cooling in the magnetic trap.

The final observation of the condensate state is done again by optical means. The atom cloud is released by switching off the magnetic field of the trap. After about 10 ms of free expansion the cloud is illuminated with resonant light and the shadow of the atomic sample is recorded by a CCD camera. In Fig. 8 we present the principle of the shadow imaging of the condensate and the image of the first BEC produced in the E. Cornell and C. Wiemann group in JILA [4].

7.1. The BEC signatures

There are distinct signatures of reaching the BEC state. They are:

- narrow peak in a velocity distribution on a broad background, indicating a qualitatively new atomic fraction,

- anisotropic shape of this peak, corresponding to the shape of the confining potential in the atomic trap, while the background has the Gaussian distribution of a thermal cloud,

- abrupt, phase-transition-like, increase in the peak's amplitude while reducing temperature.

7.2. BEC in alkali atoms

Let us summarize the characteristic features of the Bose–Einstein condensation experiments with alkali atoms which are: (i) relative simplicity of the experiment (cooling, observation), (ii) weak intra-atomic interactions (range $\sim 10^{-6}$ cm, mean distance between atoms $\sim 10^{-4}$ cm), (iii) well-known atomic structure, (iv) existence of bosonic and fermionic isotopes, e.g. ^{6}Li and ^{7}Li.

The Table presents comparison of parameters for the BEC observation in the liquid He and in alkali atoms. It clearly indicates that the alkali case is much closer to the ideal free-particle model.

TABLE

Liquid helium vs. gas BEC.

	^{4}Helium	Alkali atoms
cooling method	evaporation	rf evaporation
critical temperature [K]	0.37	0.17×10^{-6}
de Broglie wavelength λ_{dB} [Å]	30	6×10^4
density [cm^{-3}]	2.2×10^{22}	10^{14}
mean distance [Å]	3.5	1000
interaction energy [K]	20	2×10^{-10}

More details on the techniques of reaching BEC and on the condensate theory can be found in several excellent reviews, e.g., [5–7] and in the topical issue of Nature [8]. We refer also to the Nobel Lectures of the last year laureates [9].

8. Experiments with BEC

8.1. Coherent matter-wave optics

First experiments with BEC concentrated on the coherent properties of the condensate and continued the development of atom optics, demonstrated already before the advent of BEC. A property of coherent waves, well known in standard and atom optics, is their ability to interfere. Figure 9 shows the principle and results of the experiment [10], which demonstrated this property of a condensate.
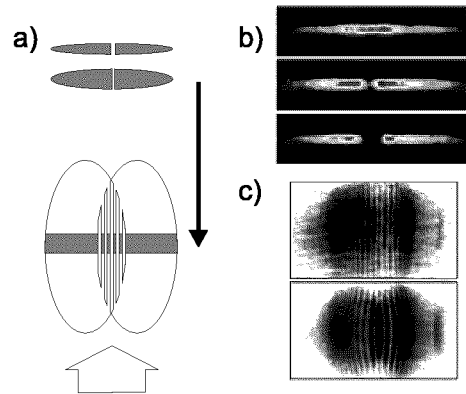

Fig. 9. (a) Observation of interference of two condensates. The condensates, released from a magnetic trap, fall down in a gravitational field (marked by a black arrow), expand due to finite initial velocities and eventually overlap. When imaged (as illustrated in Fig. 8a) the interference fringes of the atomic density can be seen. Figure (b) depicts the condensate pictures before their division and two cases of different initial separation of the divided parts. Figure (c) shows two interference patterns of the condensate density corresponding to the two initial separations (reprinted with permission from [10] — M.R. Andrews et al., "Observation of Interference between Two Bose Condensates", *Science* **275**, 637 (1997). Copyright 1997 American Association for the Advancement of Science).

Figure 9a depicts the free gravitational fall of two condensates which were produced by halving a single one. The two falling parts expand due to finite initial velocities and after some distance overlap and interfere. The observation is performed by a resonant imaging beam (block arrow) that allows recording shadow images. Figure 9b shows the initial single condensate and two separated pairs for launching them with different initial separations. Figure 9c presents two sets of interference fringes of wave matters corresponding to the two different initial
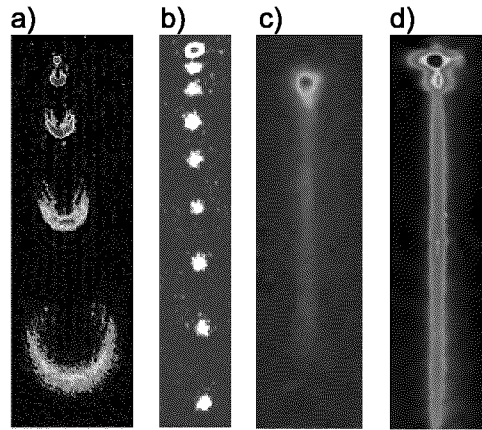
Fig. 10. Appearance of the atom-laser beams emitted by various lasers. (a) MIT laser (reprinted from Ref. [11], courtesy of W. Ketterle), (b) Yale laser (reprinted with permission from Ref. [12] — B.P. Anderson, M.A. Kasevich, "Macroscopic Quantum Interference from Atomic Tunnel Arrays", *Science* **282**, 1686 (1998); Copyright 1998 American Association for the Advancement of Science), (c) NIST laser (reprinted with permission from Ref. [13] — E.W. Hagley et al., "A Well-Collimated Quasi-Continuous Atom Laser", *Science* **283**, 1706 (1999); Copyright 1999 American Association for the Advancement of Science), (d) MPQ laser (reprinted from Ref. [14] with kind permission of the authors).

separations. The experiment is a direct analogue of the double-slit Young experiment and the matter-wave fringe period depends on the separation in exactly the same way as the light fringes depend on the slit distance in a classical version of the Young interference. Coherence of light is most spectacularly seen in laser emission. Many important applications are expected from a coherent emission of matter waves from a condensate, the "atom laser". Much effort has been devoted to demonstration of such an effect. Figure 10a presents pulses of matter waves in the first demonstration of a "pulsed atom laser" [11]. Figures 10b and c present results of improved versions built by the Yale and NIST, Gaithersburg teams [12, 13]. The laser shown in Fig. 10c allows a quasi-continuous emission, whereas that shown in Fig. 10d, from the Max-Planck-Inst. for Quantum Optics in Garching, emits a continuous matter wave [14].

8.2. Nonlinear atom optics

One important effect in nonlinear light-optics is the phenomenon of nonlinear wave mixing. Due to nonlinear response of material media to external light fields of appropriate intensity, i.e., when external light perturbation becomes comparable with intra-atomic interactions, coherent light beams are emitted from the material sample with their frequencies and directions determined by the energy
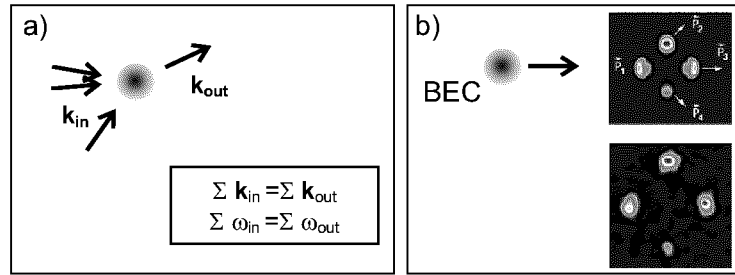
Fig. 11. Nonlinear wave mixing: (a) of light waves; (b) of the matter waves (BEC's). The top figure is a numeric simulation, the lower one shows the experimental results. Reprinted with permission from *Nature* (Ref. [15], copyright 1999, Macmillan Publishers Ltd).

and momentum conservation conditions, $\sum k_{in} = \sum k_{out}$ and $\sum \omega_{in} = \sum \omega_{out}$, where k_{in}, k_{out}, ω_{in}, and ω_{out} are the wave vectors and frequencies of the incident and emitted light waves, respectively, Fig. 11a.

In contrast to light, interaction of matter waves is always nonlinear, as governed by the last term in the Gross–Pitaevski equation describing evolution of the condensate wave function Ψ

$$i\hbar\frac{\partial\Psi}{\partial t} = \left(-\frac{\hbar^2}{2M} + V + U_0|\Psi|^2\right)\Psi, \tag{4}$$

where M is the mass of the atom, V — the external trapping potential and U_0 — the interaction coefficient. The intrinsic nonlinearity of the Gross–Pitaevski equation allows observation of nonlinear mixing also with matter waves. The upper part of Fig. 11b depicts the results of numerical simulations of such an experiment [15]. With the help of light pulses, a condensate sample is broken into three parts moving with momenta p_1, p_2, and p_3. Due to the mixing term in Eq. (4), a fourth part of condensed atoms appears and moves with momentum p_4. This is the fourth matter wave created by the nonlinear four-wave mixing process. Experimental observations shown in the lower part of Fig. 11b are in very good agreement with the simulations.

8.3. Ultra-low density condensed matter physics

Quantum-degenerate gases allow investigation of phenomena characteristic of condensed matter physics at the range of densities typical of diluted gas samples. This offers a unique opportunity of studying important processes with negligible perturbations due to mutual particle interactions. Below, we briefly discuss several examples of such possibilities.

8.3.1. Superfluidity

In the experiment of Burger et al. [16], the B–E condensate of [87]Rb atoms was placed in a magnetic trap superimposed with a 1D optical lattice. Optical

lattice is a periodic structure, created by interference of light waves of appropriate polarizations and directions. 1D lattice is the simplest case of a light wave created by two counter-propagating beams of equal polarization and frequency. Superposition of such a lattice with the magnetic trap resulted in a combined potential which consisted of a parabolic harmonic well and a sinusoidal lattice potential (the period equal to half of the optical wavelength, i.e. about 400 nm). By applying additional oscillating homogeneous magnetic field, the magnetic potential underwent periodic spatial oscillations around a given point, while the optical lattice is static (see the right frame in Fig. 12). If the temperature of the sample was above the critical value, the thermal cloud was pinned by the lattice field and did not follow oscillations of the magnetic well. However, below T_{crit}, the condensed sample (represented by darker spots in Fig. 12) moved freely and followed the oscillations of the magnetic potential. This experiment illustrates the ability of a BEC to tunnel through the potential barriers which is typical of superfluidity.
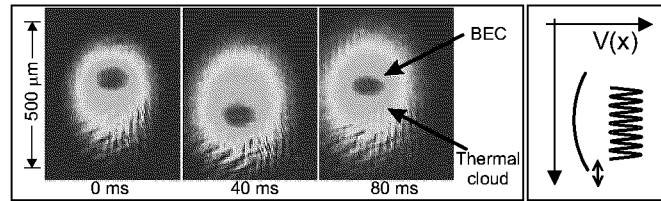

Fig. 12.   BEC (dark spots) and thermal cloud (lighter clouds) behavior in a combined potential of a harmonic well (magnetic trap) and a periodic optical lattice (seen in the right part of the figure). Spatial oscillation of a magnetic potential move the BEC across the lattice sites thanks to BEC tunnelling through the lattice barriers. The thermal cloud cannot tunnel and remains pinned by the lattice field [16, 17] (reprinted with kind permission of the authors from [17]).
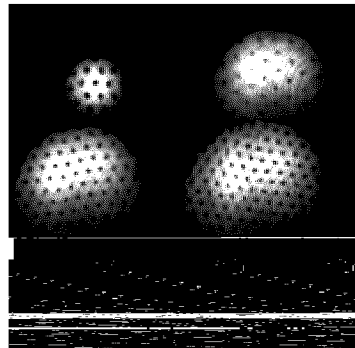

Fig. 13.   Vortice arrays in BEC created and observed by Ketterle's team (reprinted with permission from [18] — J.R. Abo-Shaeer et al., "Observation of Vortex Lattices in Bose–Einstein Condensates", Science 292, 476 (2001). Copyright 2001 American Association for the Advancement of Science).

Another phenomenon characteristic of superfluidity is creation of vortices. Figure 13 represents vortices created in the BEC sample by appropriate light fields by Abo-Shaeer et al. [17]. As in a superfluid liquid, the vortices in BEC are quantized (they carry one unit of angular momentum per vortex) and form characteristic, regular spatial arrays. Note that similarly to any other manipulation with BEC, creation of vortices can be performed exclusively by appropriate electromagnetic fields. Also, observation of the vortices is very challenging, given the size of the condensate (about 0.1 mm).

8.3.2. Josephson oscillations

Josephson oscillations with a BEC sample have been observed in the European LENS Laboratory in Florence [18]. The experiment demonstrated an oscillating atomic current in a one-dimensional array of Josephson junctions. The junction array was a 1D optical lattice superimposed on a magnetic potential trapping of the ^{87}Rb BEC. About 200 neighboring lattice sites were filled with about 1000 atoms in each well. Similarly as in another experiment on superfluidity, the optical lattice and magnetic potential could be moved independently and atomic tunnelling across the lattice potential barrier could be observed. The current of atoms tunnelling through the optical lattice barriers exhibited the oscillatory behavior typical of the Josephson effect.

8.3.3. Mott insulator

In the experiment of Greiner et al. [19], a reversible transition between the conducting (superfluid) and insulating modes has been demonstrated with BEC atoms. A 3D optical lattice has been loaded with the condensate. As long as
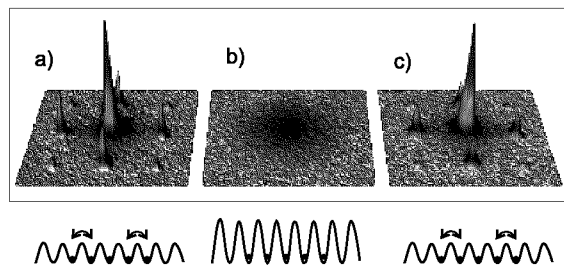

Fig. 14. BEC interference pictures demonstrating the transition between superfluid and insulating modes. A 3D optical lattice is loaded with BEC and then switched off. Atoms released from lattice sites atoms fall down and interfere. If their phases are correlated, the distinct interference pattern is seen, as in (a) and (c), while uncorrelated atoms yield a structureless distribution (b). The phase correlation depends on the lattice depth and, consequently on the atomic ability to tunnel between the lattice sites. If the lattice wells are not too deep, tunnelling is possible and an interference pattern appears, while for too deep lattice, tunnelling is prohibited and no interference structure is seen (b) (image courtesy T.W. Hänsch).

the potential depth of the lattice is low, the condensate atoms spread wave-like over the whole lattice. The atoms can move freely through the lattice potential barriers which is nothing but the superfluidity, a signature of the conducting phase. The atoms preserve strong phase correlations among themselves, so when released from the lattice and falling down due to the gravity, they can interfere and form distinct interference patterns (Fig. 14a). However, when the lattice potential is high enough, the tunneling is prohibited and atoms are localized in individual lattice sites which signifies the insulating phase (Mott insulator). Being localized in lattice wells, atoms lose their phase correlation with the consequence that no interference pattern can be seen after release from the lattice (Fig. 14b). The quantum phase transition from a superfluid to a Mott insulator is reversible, the atoms retrieve their phase correlation and return to the conducting mode when the potential barrier is lowered again (Fig. 14c). This kind of experiments allow precision study of strongly correlated systems and such effects as superconductivity. They may also find applications in quantum computing and metrology.

9. Cold fermions

Not only bosonic atoms (integer total angular momentum) but also those of fermionic character (fractional total angular momentum) can be optically cooled and trapped in magneto-optical traps. However, the quest for quantum degeneracy is much more difficult with fermionic atoms than with bosons. The reason for that is the Pauli exclusion principle which inhibits intra-fermion interaction when the de Broglie wavelength becomes comparable with the particle distances. This feature makes the evaporative cooling of fermionic atoms very inefficient at low temperatures. Fortunately, this problem can be solved by using the, so-called, sympathetic cooling which employs mixtures of bosons and fermions, or of different fermionic species, e.g., different fermionic isotopes or atoms in different spin states. Since the Pauli exclusion applies only to identical particles, the use of different atoms makes possible evaporative cooling of a given kind of atoms and their thermalization with the species of interest. In this way, by using fermionic atoms in two different spin states, Brian DeMarco and Deborah S. Jin in JILA managed to cool a gas of fermionic ^{40}K below 300 nK which is 0.5 of the Fermi temperature [20]. The onset of quantum degeneracy was seen as a barrier to evaporative cooling. Moreover, Jin and co-workers observed [21] a modification of the classical thermodynamics: the quantum degenerate fermionic atoms have energy per degree of freedom significantly higher than the $3k_{\mathrm{B}}T$ classical equipartition value (Fig. 15).

A very spectacular evidence of the Pauli blocking and the related Fermi pressure which prohibits fermionic particles from getting too close is provided by imaging the atomic clouds in temperatures corresponding to the quantum degeneracy. Randall Hulet (Rice Univ., Houston) performed such a measurement [22]
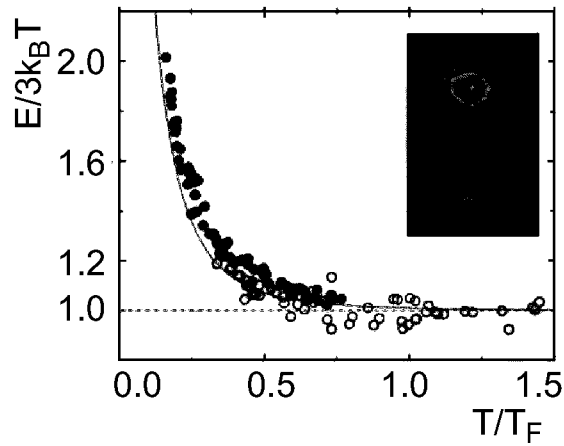
Fig. 15. Experimentally measured energy of fermionic ^{40}K atoms versus their temperature (in units of the Fermi temperature). Below T_F, a distinct deviation from the classical energy $3k_BT$ is seen [21] (reprinted with kind permission of the authors).
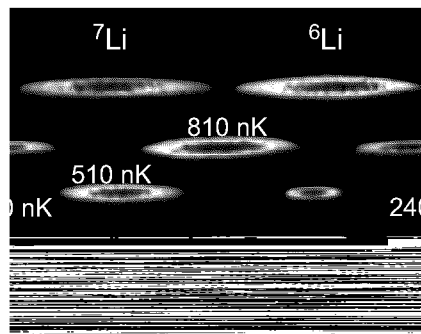

Fig. 16. Density distributions of bosonic and fermionic lithium isotopes, ^{7}Li and ^{6}Li, respectively, simultaneously trapped in the same magnetic trap. By a proper choice of laser frequency, one isotopes at a time can be imaged. When the temperature is lowered, the boson cloud decreases its size by populating lower energy states of the trap, while the fermionic cloud decreases their size much less (reprinted with permission from [22] — A.G. Truscott et al., "Observation of Fermi Pressure in a Gas of Trapped Atoms", *Science* **291**, 2570 (2001). Copyright 2001 American Association for the Advancement of Science).

with two isotopes of lithium: fermionic ^{6}Li and bosonic ^{7}Li held in the same trap under identical conditions. By using an imaging light beam of appropriate frequency, one isotope at a time has been observed. In this way the images presented in Fig. 16 have been obtained. This picture clearly demonstrates that the cloud of cold fermionic atoms cannot reach the size of the boson sample which is a direct consequence of the Fermi pressure.

10. Our way towards BEC

In Poland, experimental studies of trapped, cold atoms begun by the construction of the first MOT for rubidium atoms in the Jagiellonian University of Cracow [23]. After creation of the National Laboratory of Atomic, Molecular and Optical Physics in Toruń, we started to work towards BEC. Our design aims at condensation of ^{87}Rb atoms and consists of three main parts depicted in Fig. 17:
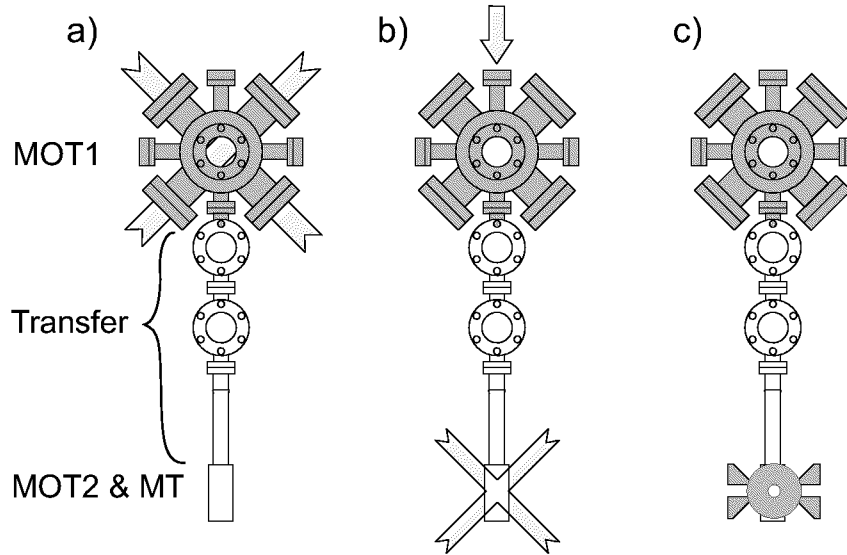

Fig. 17. The design of the Polish BEC apparatus, consisting of MOT1, the transfer part and MOT2 with the MT, and three stages of its operation: (a) MOT1 is loaded with about 10^8 ^{87}Rb atoms at about 300 μK, (b) the cold atoms are pushed down from MOT1 by a laser beam (vertical arrow) and recaptured in MOT2. (c) the laser beams are switched off and the atoms are kept in dark by MT and cooled by rf evaporation. For the sake of clarity the magnetic trap coils are shown only in (c).

(i) The first magneto-optical trap (MOT1); (ii) the transfer stage where atoms will be transported from MOT1 to the second magneto-optical trap (MOT2) and to the dark, magnetic trap (MT). The transfer needs to be done in a differentially pumped vacuum apparatus, allowing atomic passage from MOT1 region with about 10^{-8} mbar pressure to the MT region of ultra-high vacuum (about 10^{-11} mbar); (iii) MOT2 overlapping with MT. Achieving BEC will be accomplished in the following major steps:

    1. loading MOT1 and collecting a possibly large number of pre-cooled atoms (about 10^8 atoms at about 300 μK). This will be done by using laser beams (top of Fig. 17a) and quadrupole magnetic field;

2. transferring pre-cooled atoms to the lower cell by a light pressure of an extra laser beam (vertical arrow on top of Fig. 17b);

3. recapture of transferred atoms by MOT2 (in a position of MT) and cooling them below 100 μK (additional laser beams seen at the bottom of Fig. 17b);

4. magnetic trapping (three coils producing strong inhomogeneous field of the trap are shown only in Fig. 17c),

5. cooling by forced radio-frequency evaporation and thermalization by collisions below the critical temperature. In this way we expect to reach condensate of about 10^5–10^6 atoms with a critical temperature of the order of 100 nK.

11. Conclusions

In this review we aimed at a very general survey of the ideas, methods, and results of the ultra-cold atom physics. It unites the contributions from atomic physics, condensed matter physics and statistical physics. The field is rapidly developing and new, fascinating results appear every day. We refer the interested readers to the Bose–Einstein Condensation Homepage at Georgia Southern University, http://amo.phy.gasou.edu/bec.html, which gathers the most up-to-date news and contains also the BEC Online Bibliography.

Acknowledgments

References

[1] S.N. Bose, *Z. Phys.* **26,** 178 (1924).

[2] A. Einstein, *Sitz.ber. Kgl. Preuss. Akad. Wiss.* 1924, p. 261; 1925, p. 3.

[3] M.O. Mewes, M.R. Andrews, N.J. vanDruten, D.M. Kurn, D.S. Durfee, W. Ketterle, *Phys. Rev. Lett.* **77,** 416 (1996).

[4] M.H. Anderson, J.R. Ensher, M.R. Matthews, C.E. Wiemann, E.A. Cornell, *Science* **269,** 198 (1995).

[5] F. Dalfovo, S. Girogini, L.P. Pitaevskii, S. Stringari, *Rev. Mod. Phys.* **71,** 463 (1999).

[6] W. Ketterle, D.S. Durfee, D.M. Stamper-Kurn, in: *Bose–Einstein Condensation in Atomic Gases*, Eds. M. Inguscio, S. Stringari, C.E. Wieman, IOS Press, Amsterdam 1999, p. 67; arXiv:cond-mat/9904034 v2.

[7] A.J. Leggett, *Rev. Mod. Phys.* **73,** 307 (2001).

[8] *Nature* **416,** 14 March (2002) issue with review articles of: S. Chu, p. 206; J.R. Anglin, W. Ketterle, p. 211; S.L. Rolston, W.D. Phillips, p. 219; K. Burnett, P.S. Julienne, P.D. Lett, E. Tiesinga, C.J. Williams, p. 225; Th. Udem, R. Holzwarth, T.W. Hänsch, p. 233; C. Monroe, p. 238.

[9] E.A. Cornell, C.E. Wieman, *Rev. Mod. Phys.* **74,** 875 (2002); W. Ketterle, *Rev. Mod. Phys.* (2002) to be published.

[10] M.R. Andrews, C.G. Townsend, H.-J. Miesner, D.S. Durfee, D.M. Kurn, W. Ketterle, *Science* **275,** 637 (1997).

[11] D.S. Durfee, W. Ketterle, *Opt. Express* **2,** 299 (1998).

[12] B.P. Anderson, M.A. Kasevich, *Science* **282,** 1686 (1998).

[13] E.W. Hagley, L. Deng, M. Kozuma, J. Wen, K. Helmerson, S.L. Rolston, W.D. Phillips, *Science* **283,** 1706 (1999).

[14] I. Bloch, T.W. Hänsch, T. Esslinger, *Phys. Rev. Lett.* **82,** 3008 (1999).

[15] L. Deng, E.W. Hagley, J. Wen, M. Trippenbach, Y. Band, P.S. Julienne, J.E. Simsarian, K. Helmerson, S.L. Rolston, W.D. Phillips, *Nature* **398,** 218 (1999).

[16] F.S. Cataliotti, S. Burger, C. Fort, P. Maddaloni, F. Minardi, A. Trombettoni. A. Smerzi, M. Inguscio, *Science* **293,** 843 (2001).

[17] F. Ferlaino, P. Maddaloni, S. Burger, F.S. Cataliotti, C. Fort, M. Modugno, M. Inguscio, *Phys. Rev. A* **66,** 011604R (2002).

[18] J.R. Abo-Shaeer, C. Raman, J.M. Vogels, W. Ketterle, *Science* **292,** 476 (2001).

[19] M. Greiner, O. Mandel, T. Esslinger, T.W. Hänsch, I. Bloch, *Nature* **415,** 39 (2002).

[20] B. DeMarco, D.S. Jin, *Science* **285,** 1703 (1999).

[21] B. DeMarco, S.B. Papp, D.S. Jin, *Phys. Rev. Lett.* **86,** 5409 (2001).

[22] A.G. Truscott, K.E. Strecker, W.I. McAlexander, G. Partridge, R.G. Hulet, *Science* **291,** 2570 (2001).

[23] J. Zachorowski, T. Pałasz, W. Gawlik, *Opt. Appl.* **28,** 239 (1998).